Three-Dimensional Modeling and Kinematic Analysis of Human Elbow Joint Axis Based on Anatomy and Screw Theory

Yongsheng Gao, Guodong Lang, Wenpeng Shen, and Jie Zhao

***Abstract*—Ensuring the motion consistency of human and exoskeletons is the key to the research of wearable exoskeleton robots. However, as the complexity of the coupling of sliding and rolling motion in human joint tissue, it is hard to depict the dynamic states of the joint axis. Exploring the changed human joint axis can be significant in the process of studying the bionic joint of the exoskeleton robots. We proposed a method to build the biological joint model based on anatomy and used screw theory to explore the human biological joint axis on it. The humerus and ulna models were only reconstructed by scanning CT images of the elbow joint in any single position. According to anatomy, humerus trochlear and trochlear notch of models were tangent to build a movable elbow joint model. The screw theory was used to study the elbow joint axis based on the kinematic data of samples in the motion simulation of joint model. Comparing the motion between model and human experiment, the R^2 of the Euler angles were above 0.97, and $RMSE$ were below 2.85, which showed the model following anatomical principles can reflect the human joints well. And the pattern that depicted joint axis travelled is similar to the shape of the Mobius Strip. This work provides a new method to study human joint axis, and the axis results provide references to the design of exoskeleton joints and bionic robots.**

***Index Terms*—Biomimetics, human and humanoid motion analysis and synthesis, human joint axis, screw theory, wearable robotics.**

I. INTRODUCTION

WEARABLE exoskeleton robots have received considerable attention as a technical means to enhance human movement ability and improve the quality of human life [1], [2]. They can provide extra power for humans to overcome their own physical limitations, such as effective neurorehabilitation training for patients with abnormal nerve connections, limb injuries, etc, to promote sports recovery [3], [4], [5], [6]. However, the exoskeletons are a kind of human-machine coupled equipment, and human motion is complex process, and joint rotations are the results of the interaction between neurons, muscles, and bones [7]. Placing the exoskeleton robots in parallel with the complex biological joints and making the exoskeletons fit the human motion is a significant challenge [8].

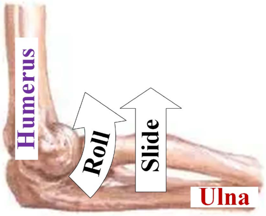

Fig. 1. Sliding and rolling between the humerus and ulna under the trochlear structure.

The joints of exoskeleton robots are composed of linear and rotational mechanisms with mechanical manufacturing. However, the main joints of the human body are the trochlear joints, which has been proved to be complex motion with biological characteristics coupled with sliding and rolling [9], [10], as shown in Fig. 1. Ensuring the motion consistency of robot joints and human joints is the key to the research of wearable exoskeleton robots. In order to adapt to the movement of the limbs, the researchers proposed solutions from several aspects. Some researchers proposed to increase the number of joints of exoskeleton robots to match the motion space of the limbs under the joint motion [11], [12], [13]. These methods lead to redundant structure of the exoskeleton, which do not fit human body and are also difficult to control. Other researchers used advanced control theories such as Adaptive Gait Pattern, Proportional Electromyography Control, and Human–Machine Interface to control the exoskeletons to conform to the joint motions as much as possible based on the mechanical structure of joints [1], [13], [14]. Due to the inconsistency of joint structures of human and robots, the ability to reduce interaction forces is limited. The above methods have insufficient understanding of complex human joints, so that they cannot truly break through the technical problems of human-machine coupling. Exploring the real motion laws of joints is of great significance for designing compact exoskeletons that meet the characteristics of human-machine coupling.

The elbow joints are typical trochlear joints. The humerus and ulna roll and slide under the trochlear structure, and the movement between them is not in the same plane thanks to the carrying angle. In this case, the joint axis could be regarded to change all the time in space, so it is difficult to accurately study the real

---

Manuscript received 2 May 2022; accepted 3 September 2022. Date of publication 9 September 2022; date of current version 15 September 2022. This letter was recommended for publication by Associate Editor X. Liu and Editor J. Zhao upon evaluation of the reviewers' comments. This work was supported by the National Key Research and Development Program of China under Grant 2018YFB1307801. *(Corresponding author: Guodong Lang.)*

The authors are with the State Key Laboratory of Robotics and System, Harbin Institute of Technology, Heilongjiang 150000, China (e-mail: gao_ys@126.com; 1031383936@qq.com; swp1064828377@163.com; jzhao@hit.edu.cn).

Digital Object Identifier 10.1109/LRA.2022.3205547

three-dimensional motion law of the joints. Some researchers used the marking method to embed markers on the bone and skin surface, and measured the movement of several markers to analyze the joint motion [15], [16], [17]. These methods are based on the assumption that the movement of the markers truly reflects the joint motion. But elastic deformation occurs between skin, muscle and bone. And the fixation of the marker will affect the physical state of the joint and change the natural kinematics. These factors can affect the accuracy of the measurements. Some researchers proposed motion capture methods without markers [18], [19]. The camera collected human motion data, and machine learning was used to identify features, and joint motion was analyzed based on limb features. These methods can measure non-invasively, but the recognition of dynamic features by machine learning in videos is unstable and the recognition accuracy is limited. The above two types of methods both study the rotation of the entire joint through several measurement points, without in-depth analysis of the motion structure and mechanism. Other researchers proposed non-invasive scanning methods [9], [20], which collected CT/ MRI data of joints at multiple locations, and measured the changes of bone features, and used fitting or approximation methods to find the joint axis. This kind of methods can acquire the accurate static states of joints, but cannot acquire the dynamic states of joints. The accuracy of the axis depends on the scanning frequency, and the fitting and approximation methods have errors with the actual situation in principle. Due to the special structure of biological joints, joint analysis relies on human experiments, and there is currently no joint model that can demonstrate rotation in vitro.

As for our work, biomechanical modeling has advanced, but exploration of joint kinematics remains a challenge., the kinematics has evolved from simple bending and hinges to more complex surfaces and spatially parallel mechanisms. The study of the elbow joint axis has evolved from flexion occurred at the center of the skeletal spherical surface [21], to that the joint axis change was a three-dimensional motion [17]. Until now, the elbow joint axis change is a vortex-like shape [20]. These conclusions are drawn on the basis of fitting the kinematic data, and there are errors with the actual joint axes in calculation principle. Analyzing the mechanism of joint rotation based on the biological structure of the bones in the joint will greatly facilitate the exploration of the complex motion law of the joint. According to anatomy, in the trochlear structure of the joint, there is a groove in the middle of the joint socket, and the sagittal crest of the joint head, they cooperate to roll and slide under the lubrication of the cartilage. The three-dimensional reconstructed humerus and ulna models can be creatively assembled into movable joint models according to anatomy. On the other hand, the changing joint axis under complex motion is challenging. In the field of robotics, screw theory describes the general motion in space with a spiral, which is mostly used to solve the pose transformation of robots [22]. The axis parameters in the screw have great advantages for calculating joint axis. And in the principle of calculation, the error of the screw method is very small, and it is more accurate than the method of approximation and fitting.

In this paper, we took the right elbow joint aixs as the research object, and proposed a method to build a movable joint model in vitro based on anatomy and CT scanning, and to calculated the joint axis based on screw theory. It only needs to scan the CT data of the elbow joint at one position, and reconstruct three-dimensional models of the humerus and ulna. And the models of humerus and ulna could be connected according to the anatomical structure which humeral trochlear and unlar trochlear notch of models are tangent, which could form a movable joint model, which could dynamically analyze the three-dimensional movement of the elbow joint in the natural state. Then the screw theory could be used to study the elbow joint axis based on the kinematic data of samples in the motion simulation of joint model.

This modeling method inherits the precise advantages of CT/ MRI scanning method, and also has the advantages of dynamic analysis of motion tracking technology, and truly restores the motion mechanism of the elbow joint in vivo, which has been verified by human experiments. The method of axis calculation can more accurately explore the complex axis of the biological joint. They provide a new idea for solving the axis of other biological joints. The results of studying the joint axis provide a reference for designing exoskeleton robot joints and improving human-robot coupling performance.

II. Materials and Method

In this section, first, the CT data of the elbow joint was acquired. Then, the humerus and ulna models were reconstructed in three dimensions, and they were assembled according to anatomical principles to build movable joint model. After that, the method of finding the joint axis was described using the screw theory.

The research was carried out following the principles of the Declaration of Helsinki.

A. *Material Acquisition*

For obtaining the CT datas of the human elbow joint, we recruited a volunteer who is 24 years old with healthy joints. The Toshiba's Aquilion ONE Spiral CT Machine provided by the Department of Radiology, Harbin Institute of Technology University Hospital, was used to scan the volunteer's right elbow joint. The parameters of it are as follows: the ray tube voltage is 120 kV, the thickness between adjacent slices is 2 mm, the resolution is 512×512, and the pixel pitch is (0.469, 0.469). During the scanning process, the human body was in a prone position, the fixed arm was in an extended state, as shown in Fig. 2, and the CT images as shown in Fig. 3. The 240 processed elbow CT images were used to reconstructed three-dimensional models of humerus and ulna.

B. *Modeling the Elbow Joint*

In order to build an independent moveable joint model that can reflect the actual motion, we followed the principle of humeral and ulnar trochlear notch rolling and sliding insread of the fixed axis.

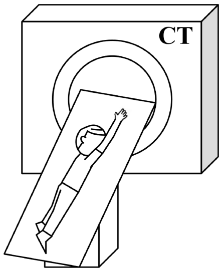

Fig. 2. Human posture in CT scanning.

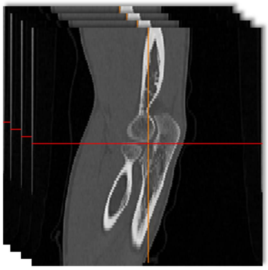

Fig. 3. CT images of elbow joint.

First, we should mark the key features of humerus and ulna, as shown in Fig. 6. So we drew out curves of the humeral trochlear and ulnar trochlear notch, which two marked parts should be tangent to each other. The coronoid fossa anterior to the coronal plane and the olecranon fossa posterior to the coronal plane in humerus and the coronoid anterior and the olecranon posterior in ulna were also marked out.

Next, we should connect humerus with ulna to build elbow model.

When there is only one tangent point on curves, the free degree of the model is too high to stable the movement, and it does not conform the law of motion. When there are two tangent points as shown in Fig. 4, the two points are located at the front and back of the coronal plane (with the coronal plane as the boundary). It is obvious that the degree of freedom reduced would help to consistent with the law of motion.

Even though there are two tangent points, the possibility of how they touch each other would be uncertained, as shown in Fig. 5. They should be constrained according to the characteristics of the trochlear joint structure, as the plane formed by the Z-axis and X-axis of the ulnar coordinate should be constrained to be parallel to the sagittal plane of the human body.

There should be a certain range of flexion and extension of the elbow joint. The contact between the olecranon and the olecranon fossa and the contact between the coronoid process and the coronoid fossa were used the limiting positions, and the joint was extended to an upper limb model, as shown in Fig. 7.

After that, we should simulate the motion of the upper limb model. Since the constructed upper limb model was set as an incompressive rigid body, a point on the forearm of the model was selected as a virtual marker to record the movement data as shown in Fig. 8.

C. The Method of Calculating the Joint Axis

In this part, the movement datas in last part were used to calculate the joint axis by screw theory.

1) The Basics of Screw Theory: Lie group is a group with continuous (smooth) properties [22]. A rigid body moves continuously in space, its movement can be regarded as a special Lie group $SE(3)$, can be expressed as:

$$SE(3) = \left\{ \begin{bmatrix} \boldsymbol{R}\, \boldsymbol{p} \\ 0 \;\; 1 \end{bmatrix} | \boldsymbol{R} \in SO(3), \boldsymbol{p} \in \mathbb{R}^3 \right\} \tag{1}$$

Where $SO(3)$ is a special orthogonal group and $\boldsymbol{R}$ can be used to describe rotational motion in three-dimensional space. The antisymmetric matrix $\boldsymbol{p}$ is used to describe translational action.

Lie algebra is an algebraic tool for studying Lie groups [21]. The Lie algebra of $SE(3)$ is denoted $se(3)$, and the Lie algebra of $SO(3)$ is denoted $so(3)$.They are exponential mapping and logarithmic mapping to each other respectively.

Screw is the element of the projective Lie algebra, which can be expressed as:

$$\begin{aligned} \boldsymbol{S} &= \begin{pmatrix} \boldsymbol{s} \\ \boldsymbol{s_0} \end{pmatrix} = \begin{pmatrix} \boldsymbol{s} \\ \boldsymbol{r} \times \boldsymbol{s} + h\boldsymbol{s} \end{pmatrix} \\ &= (s_x, s_y, s_z, s_{x0}, s_{y0}, s_{z0})^T \end{aligned} \tag{2}$$

Where the screw includes two parts, the axis vector $\boldsymbol{s} = (s_x, s_y, s_z)^T$ is the main part, the vector $\boldsymbol{s_0} = (s_{x0}, s_{y0}, s_{z0})^T$ is the dual part, the vector $\boldsymbol{r}$ is the position vector of the axis, the screw pitch h is the projection of the dual part in the main,

Using screw to describe the rigid body motion, which can be expressed as:

$$e^{[\boldsymbol{S}]\theta} = \begin{bmatrix} \boldsymbol{R} & \boldsymbol{p} \\ 0 & 1 \end{bmatrix} \tag{3}$$

where

$$[\boldsymbol{S}]\,\theta = \begin{bmatrix} [\boldsymbol{\omega}]\,\theta & \boldsymbol{v}\theta \\ 0 & 0 \end{bmatrix} \in se(3) \tag{4}$$

Where $\boldsymbol{S}$ is the screw axis, $\boldsymbol{R}$ is the rotation matrix, $\boldsymbol{p}$ is the translation matrix, θ is the angle of screw, $[\boldsymbol{\omega}]$ is the angle velocity matrix, $\boldsymbol{v}$ is the linear velocity.

2) Calculation of Joint Axis Based on Screw Theory: Make a marker on the forearm of the constructed upper limb model and record the position and orientation datas of marker during the elbow flexion and extension. As the model is a rigid body, the datas can directly reflect the movements of elbow.

Taking two sampling data at adjacent intervals as $\boldsymbol{m_i}, \boldsymbol{m_{i+1}}$, which can be expressed as:

$$\boldsymbol{m_i} = (x_i, y_i, z_i, \alpha_i, \beta_i, \gamma_i)^T \tag{5}$$

$$\boldsymbol{m_{i+1}} = (x_{i+1}, y_{i+1}, z_{i+1}, \alpha_{i+1}, \beta_{i+1}, \gamma_{i+1})^T \tag{6}$$

where the x_i, x_{i+1}, y_i, y_{i+1}, z_i, z_{i+1} are the parameters of position. The α_i, α_{i+1}, β_i, β_{i+1}, γ_i, γ_{i+1} are the Euler angles.

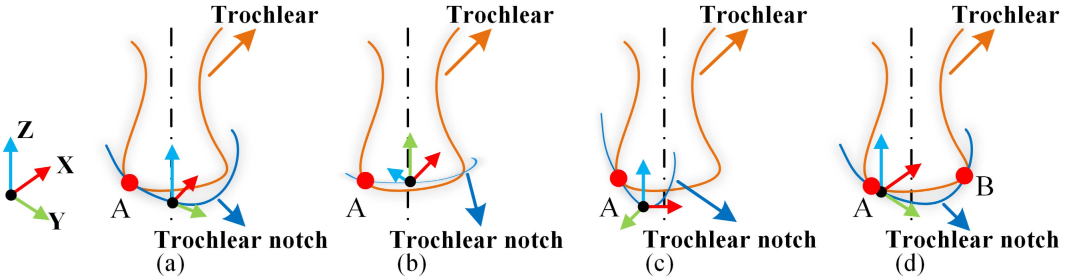

Fig. 4. Connection of tangent points.The red dots(A, B) are the tangent points. The reference coordinate in the left is the Human Body Coordinate. The dot-and-dash line is the boundary of coronal plane. (a) A proper place which the orientation of trochlear notch correspond with reference coordinate system on the left. (b) The orientation rotates along X-axis from (a). (c) The orientation rotates along Z-axis from (a). (d) A proper place which has double tangent points.

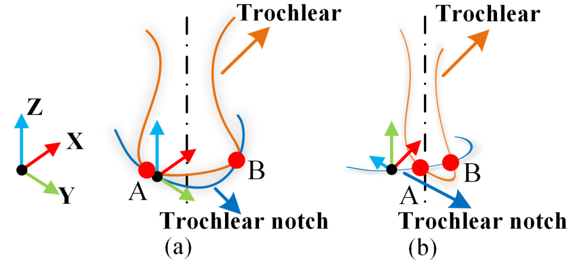

Fig. 5. (a) is a suitable tangent situation, (b) is a situation where the pulley happens to twist.

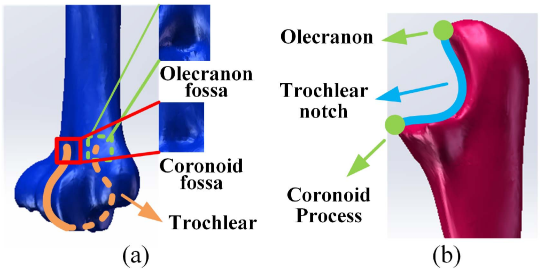

Fig. 6. (a) The red framed area of the humerus is the coronoid fossa, the green framed dot is the olecranon fossa, and the orange curved line is marked as the trochlear. (b) The upper green area of the ulna is the olecranon, the lower green area is the coronoid process, and the blue curved line is marked as the trochlear notch.

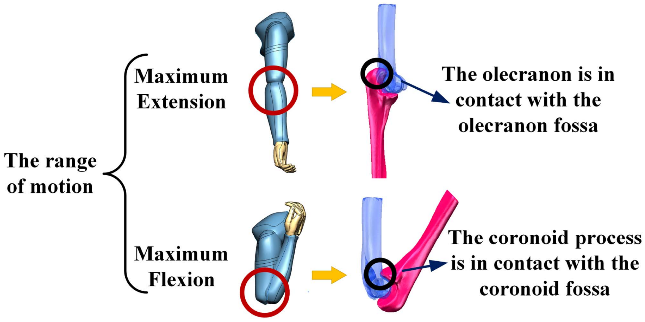

Fig. 7. The limiting positions of elbow flexion and extension.

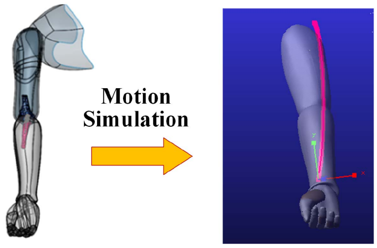

Fig. 8. The motion simulation of upper limb model.

The homogeneous transformation matrix of position and orientation $\boldsymbol{T}$ can be expressed as [23]:

$$\boldsymbol{T} = \begin{bmatrix} c\alpha c\beta & c\alpha s\beta s\gamma - s\alpha c\gamma & c\alpha s\beta c\gamma + s\alpha s\gamma & x \\ s\alpha c\beta & s\alpha s\beta s\gamma + c\alpha c\gamma & s\alpha s\beta c\gamma - c\alpha s\gamma & y \\ -s\beta & c\beta s\gamma & c\beta c\gamma & z \\ 0 & 0 & 0 & 1 \end{bmatrix} \tag{7}$$

where the s represents $sin\theta$, the c represents $cos\theta$. According to (7), $\boldsymbol{T_i}$, $\boldsymbol{T_{i+1}}$ are calculted by $\boldsymbol{m_i}$, $\boldsymbol{m_{i+1}}$.

Taking $\boldsymbol{S_i}$ as the screw axis between $\boldsymbol{T_i}$ and $\boldsymbol{T_{i+1}}$, and screw motion is used for describing the motion between them, as follows:

$$\begin{aligned} e^{[\boldsymbol{S}_i]\theta_i} &= \boldsymbol{T_{i+1}T_i^{-1}} \\ &= \begin{bmatrix} e^{[\boldsymbol{\omega_i}]\theta_i} & \left(\boldsymbol{I}\theta_i + (1-\cos\theta_i)[\boldsymbol{\omega_i}] + (\theta_i - \sin\theta_i)\,[\boldsymbol{\omega_i}]^2\right)\boldsymbol{v_i} \\ 0 & 1 \end{bmatrix} \end{aligned} \tag{8}$$

where θ_i is the screw angle of $\boldsymbol{S_i}$, $[\boldsymbol{\omega_i}]$ is the angular velocity matrix, $\boldsymbol{v_i}$ is the linear velocity vector.

According to the Rodrigues's formula, the rotating part of the screw motion $\boldsymbol{S_i}$ can be expressed as:

$$\begin{aligned} Rot(\boldsymbol{\omega_i}, \theta_i) &= e^{[\boldsymbol{\omega_i}]\theta_i} \\ &= I + \sin\theta_i\,[\boldsymbol{\omega_i}] + \left(1 - \cos\theta_i[\boldsymbol{\omega_i}]^2\right) \in SO(3) \end{aligned} \tag{9}$$

Combining with (3), (8) and (9), let $R_i = Rot(\boldsymbol{\omega_i}, \theta_i)$, $\boldsymbol{\omega_i}$ and θ_i are calculated, and it tells the direction and rotation angle of joint axis.

Combining with (3) and (8), the $\boldsymbol{v_i}$ can be calculated by the following formula:

$$G^{-1}(\theta_i) = \frac{1}{\theta_i} I - \frac{1}{2}[\boldsymbol{\omega_i}] + \left(\frac{1}{\theta_i} - \frac{1}{2}\cot\frac{\theta_i}{2}\right)[\boldsymbol{\omega_i}]^2 \tag{10}$$

$$\boldsymbol{v_i} = G^{-1}(\theta_i)\,\boldsymbol{p_i} \tag{11}$$

So far, $\boldsymbol{\omega_i}$, θ_i and $\boldsymbol{v_i}$ are all calculated, and the screw motion $\boldsymbol{S_i}$ can be determined.

Further, according to (2), the position vector $\boldsymbol{r_i}$ and the screw pitch h_i of $\boldsymbol{S_i}$ can be calculated as follows:

$$\boldsymbol{r_i} = \frac{\boldsymbol{s_i} \times \boldsymbol{s_{i_0}}}{\boldsymbol{s_i} \cdot \boldsymbol{s_i}} \tag{12}$$

$$h_i = \frac{\boldsymbol{s_i} \cdot \boldsymbol{s_{i_0}}}{\boldsymbol{s_i} \cdot \boldsymbol{s_i}} \tag{13}$$

where $\boldsymbol{r_i}$ indicates the positoin of the joint axis, h_i indicates the linear distance that the forearm body translates along the joint axis.

In addition, The entire change of the joint axis can be recorded by the parametric equation. The axis of each moment can be written as $\boldsymbol{S_t} = (x_t, y_t, z_t, \alpha_t, \beta_t, \gamma_t, \boldsymbol{r_t}^T, h_t)^T$, and the calculation formula is as follow:

$$\boldsymbol{S_t} = \boldsymbol{A}t^2 + \boldsymbol{B}t + \boldsymbol{C} \tag{14}$$

Where $\boldsymbol{A}$, $\boldsymbol{B}$, $\boldsymbol{C}$ are undetermined coefficient matrices.

III. EXPERIMENTS AND RESULTS

In this section, the simulation of the joint model was compared with the natural motion of human joints to verify the validity of the model. Then, the joint axis calculated by the screw method was displayed. And then, the law of the joint axis was analyzed and explored.

A. *The Elbow Joint Model Evaluation*

In order to verify the validity of the model, it is necessary to carry on the experiments on human subjects and then compare them with the model motion. The wearable markers limit the movement, and would result in inaccuracy of meansurement. To prevent this, we measured the movement of when an object was being moved while the elbow was flexing to ensure the upper limb was in a natural state. Also it is hard to be placed at a position between the object marker and simulation markers, but the orientation of them are changing as the same, which can be used to compare to verify the validity.

The volunteer held the inertial measurement unit (IMU) with positioning his/her wrist and upper arm still, as shown Fig. 9. The volunteer did flexion and extension exercises three times. The motion datas of volunteer were compared with the simulation of model.

The results are shown in Fig. 10. The motion in the model simulation are almost matching the results of human motion, which mean that the simulated motion of the model could reflect the real motion of human subject.

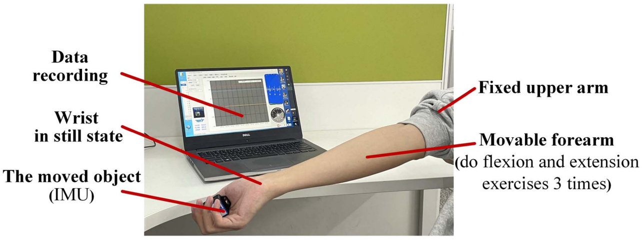

Fig. 9. Experiments on human subject.

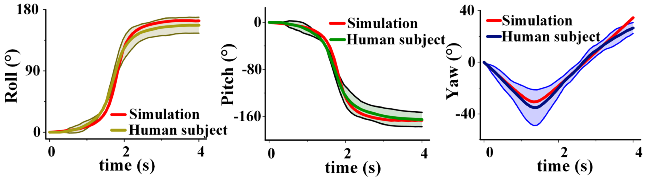

Fig. 10. Comparison of Euler angles between model simulation and human subject. The shaded area is the error band.

TABLE I
$RMSE$ AND R^2 IN EULER ANGLES

	Roll	Pitch	Yaw
$RMSE$	1.40	2.85	2.34
R^2	0.993	0.971	0.982

Root Mean Square Error($RMSE$) and R^2 between the average Euler angles of the results of the human subject and the model simulation are shown in Table I.It could be seen from the Table I that the biggest difference is in the Pitch, but the overall R^2 of the model is above 0.971 and $RMSE$ are below 2.85, which also shows that the elbow joint model is more consistent with the actual human body joint motion.

B. *The Results of Calculating Joint Axis*

The axis was calcuated by screw theory as shown in Fig. 11. The joint axis moved in a space of (0.5, 0.15, 0.15)mm in a roundabout way. We could see that the changes in the axis position and orientation were mapped to an irregular shape in space. According to the characteristics of the changing axis, we divided it into three states, as shown in Fig. 12.

The current methods of studying joint motion only measure the motion representation directly, such as the change of the elbow joint visually or the change of the markers. In this paper, the screw theory is used to calculate the axis of the actual movement of the elbow joint. This is a new method for studying the complexion of the axis of joint motion under the physiological structure and contributing to the research in sports science.

C. *The Analysis of Joint Axis Law*

It needs eight screw parameters to describe the changes of the joint axis all at once, including three position parameters, three orientation parameters, pitch angle, and pitch.

In term of the position change, curvature K and torsion T were calculated from the changes of the axis's position, as shown in Fig. 13(a), (b). The pitch angle and the pitch are shown in

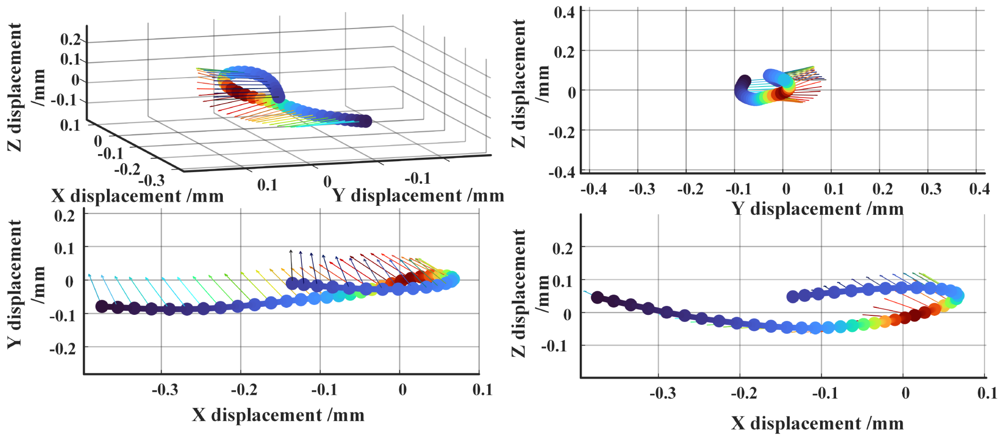

Fig. 11. The change of joint axis. The four pictures represent different views. The dots in the figures represent the position of the axis, the color of the dots represents the helix angle of the screw, and the angle range is 0-15. The arrows represent the orientation of the joint axis, and the color of arrows represent the pitch angle, and the pitch range is $(-0.1889, -0.0349)$ mm/rad.

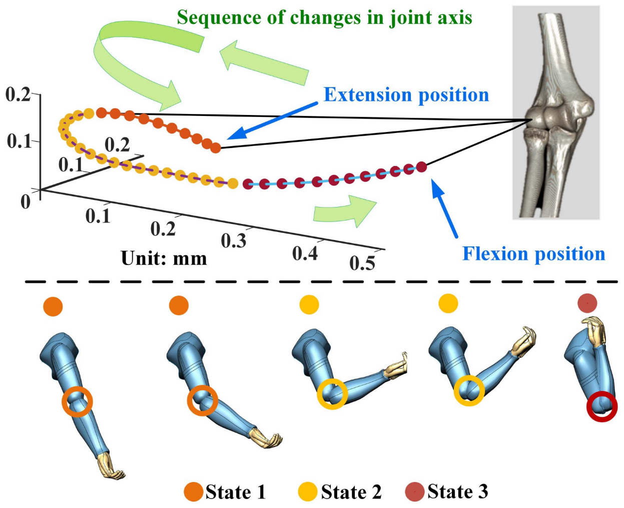

Fig. 12. Three states of elbow under the influnce of joint axis changes. The dots are the positions of joint aixs. The lines are the sequence of changes in joint aixs. The color of circles in joints below shows the states of elbow.

Fig. 13(d), (e). From the information above, the characteristic of the change of the joint is obvious in State 2 (Fig. 12). This proves that the robots can not coordinate with the human's movement when wearing the articulated exoskeleton.

The quaternion could use to describe the orientation of axis. Geodesics in the Quaternion manifold could be used to measure the surface distance between each axis to describe the change in orientation. The formula is as follow:

$$dist = p_1 p_2^{-1} \tag{15}$$

where p_1 and p_2 is the orientations of two adjacent axes in form of quaternion.

The distances are shown in Fig. 13(c). And the orientation were mapped on the unit sphere, as shown in Fig. 14. And the trace of the orientation forms a curved triangle on the unit sphere.

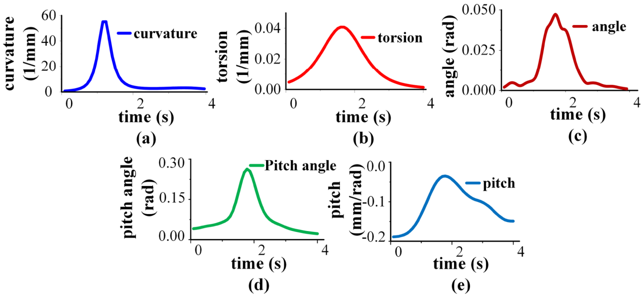

Fig. 13. (a) is the curvature of the axis trace; (b) is the torsion of the axis trace; (c) is the Geodesic distance; (d) is the change of pitch angle; (e) is the change of picth.

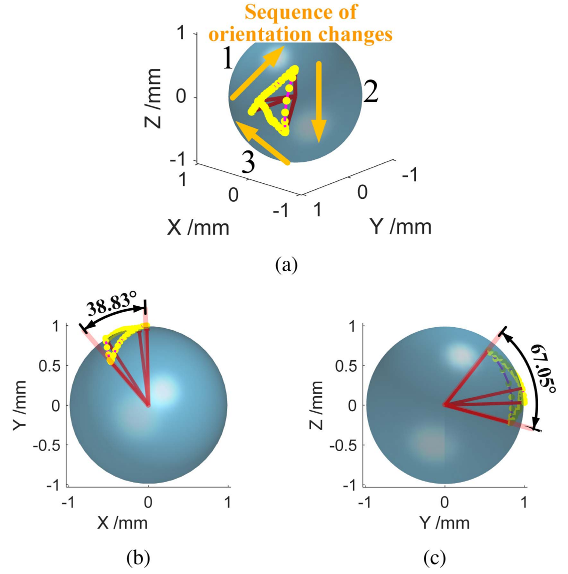

Fig. 14. The change of orientation. (a) The direction of the arrow represents the direction of orientation change, and the serial number indicate the order of the three sides of the curved triangle. (b) Its orientation changes 38.83° around the vertical axis of human body. (c) Its orientation changes 67.05° around the sagittal axis.

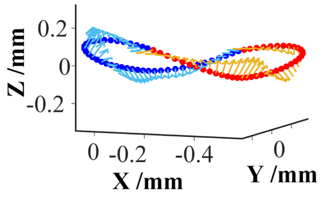

(a) (b)

Fig. 15. The blue dots and arrows represent the actual axis of the elbow joint, and the red dots and arrows represent the auxiliary graphics for the symmetry and rotation of the actual elbow joint axis.

Its orientation changes 38.83° around the vertical axis of human body, and 67.05° around the sagittal axis.

In order to further expanding the trend that shows the change of the joint axis to find the complete pattern,firstly we copied the figures, then we made a symmetrical and rotational transformation to splice it with the original figure, as shown in Fig. 15. Two parts can form like Mobius Strip in shape, which has a special structure and has only one face in three-dimensional space. It is also similar to the symbol '∞'.

IV. DISSCUSSION

A. *Comparison With Existing Methods for Motion Analysis*

At present, the main analysis methods of joint motion include marking method, motion capture method and CT/MRI static scanning. Ayman Assi et al. [16] used the marking method to measure the flexion and extension of the elbow joint multiple times, and its Intraclass Correlation Coefficient (ICC) $= 0.42$, while ICC > 0.6 to regard the movement as moderately high reliability. As the joint bent, displacement and deformation occured between the skin, tissue, and bone, resulting in inaccurate measurements. And markers also limited the natural motion of the limbs. Aouaidjia Kamel et al. [18] used a motion capture method based on image recognition, and the similarity rate of overall actions was over 70%, and the best similarity rate was 94%. But feature recognition in video is unstable. Both the marking method and the motion capture method are based on several measurement points, which are not enough to show the changes in the structural features of the joints. Michele Conconi et al. [24] used CT/ MRI static scans to calculate the complex motion of the trochlear joint with a rotational angle error of 2.2°. It could acquire the morphology of static joints in vivo non-invasively and accurately, but could not perform dynamic analysis. The above existing methods all have the limitations of not being able to dynamically display the mechanism of joint motion and measure the natural state.

The work of this paper innovatively combined the ideas of anatomy and mechanical assembly, breaking through the limitations of the existing methods. The three-dimensional reconstructed humerus and ulna models were assembled together to build a model outside the human body to reproduce the coupled motion mechanism of sliding and rolling inside the joint. The model could reflect the natural motion of the joint, which could be used for measurement motion and research analysis.

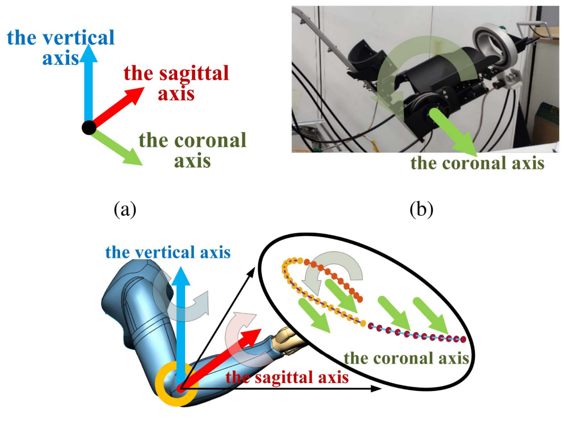

(a) (b)

(c)

Fig. 16. (a) is the human coordinate system; (b) is the movement of the exoskeleton of fixed joint axis; (c) is the movement of human body.

After comparing the model results with human experimental data, the R^2 of angles were above 0.97, and $RMSE$ were below 2.85 (refer to Table I), which verified the validity of the model. And this is a non-invasive method, it does not require invasive marking on the human body, which avoid harm to people.

For the law of joint axis change, Arnold Adikrishna et al. [20] fit the motion data and used the parametric equation method to explain that the elbow joint was a vortex-like shape. The fitting method has errors between model and the actual from the calculation principle. In this study, the screw method was applied to the motion data to calculate the axis change of the elbow joint. Its shape is similar to half of '∞,' and the change trend is in line with the Mobius Strip. In terms of the direction change of the axis, the changing shape forms a curved triangle on the unit sphere. From the calculation principle, there is almost no error in using the screw to calculate the change of the complex joint axis.

B. *The Significance of the Study for Exoskeleton*

The conclusion of the joint axis in this paper will provide an important reference for exoskeleton design and other robot researches that involve the human motion. In the field of exoskeletons, there are mismatching between the human and robots in relation to the complexity of human joint motion when the exoskeletons are worn. Taking the elbow joint as an example, the forearm of exoskeleton usually would rotate around the motor axis parallel to the coronal axis of human body. But the human forearm would also rotate slightly about 38.83° around the vertiacl axis, and about 67.05° around the sagittal axis. The joint axis would also moves in a space of (0.5, 0.15, 0.15)mm in a roundabout way, as shown in Fig. 16. With the research method and results mentioned as above, we can explain the specific reasons for the mismatching of axes in detail. Refering this law of human joint motion, researchers could design exoskeleton joint with bionic structure which will contribute to the coordination and synchronization with human body movement.

C. Prospects for the Future Work

In terms of modeling, this is still a simplified model, because the method is based on the special physiological skeletal structure of joints, but ligaments in actual. Different ligaments produce pulling forces, which will cause the connected joints to deviate slightly under the condition of satisfying the matching relationship. Therefore, in order to further understand the human joints, the next step could be to consider the influence of ligaments and other tissues on joint movement. As we known, ligaments are elastic band-like structure. When adding ligaments and other elastic tissues, not only their positions to connect with the bone, but also their material mechanical properties should be considered. This is a difficult but instructive work for understanding the joints of living organisms and the design of future robot kinematics. The rigid structure of bones and elastic structures such as ligaments and cartilage together form the joint structure of the human body. When designing an exoskeleton robot, this idea can also be referred to. The carry body part could be designed as a rigid structure, and the body connected part could be designed to have an elastic structure.In this way, the coupling between the complex motion of the human body and the motion of the robot can be realized better.

V. CONCLUSION

In this study, we proposed a kinematic model, through which the natural motion of the human joint was studied. It only needs to scan the CT data of the elbow joint at one position, and reconstruct three-dimensional models of the humerus and ulna. The models of humerus and ulna were connected according to the anatomical structure which humeral trochlear and unlar trochlear notch of models were tangent, which formed a movable joint model. And on the basis of model, the screw theory was used to calculate the changing joint axis. The research showed the trend of changing axis conformed a shape as a part of Mobius Strip. This method provids a reference for the early diagnosis of elbow diseases and the design of medical rehabilitation equipment by revealing the changing pattern of the axis of the elbow joint during movement. Referring to the conclusion of joint axis, researchers could design servo robotic joints to adapt the change of axis, further improving man-machine coupling performance.

REFERENCES

[1] K.-W. Park, J. Choi, and K. Kong, “Iterative learning of human behavior for adaptive gait pattern adjustment of a powered exoskeleton,” *IEEE Trans. Robot.*, vol. 38, no. 3, pp. 1395–1409, Jun. 2022.

[2] G. Durandau, W. F. Rampeltshammer, H. v. d. Kooij, and M. Sartori, “Neuromechanical model-based adaptive control of bilateral ankle exoskeletons: Biological joint torque and electromyogram reduction across walking conditions,” *IEEE Trans. Robot.*, vol. 38, no. 3, pp. 1380–1394, Jun. 2022.

[3] S. V. Sarkisian, M. K. Ishmael, and T. Lenzi, “Self-aligning mechanism improves comfort and performance with a powered knee exoskeleton,” *IEEE Trans. Neural Syst. Rehabil. Eng.*, vol. 29, pp. 629–640, 2021.

[4] E. P. Washabaugh, T. E. Augenstein, A. M. Ebenhoeh, J. Qiu, and C. Krishnan, “Design and preliminary assessment of a passive elastic leg exoskeleton for resistive gait rehabilitation,” *IEEE Trans. Biomed. Eng.*, vol. 68, no. 6, pp. 1941–1950, Jun. 2021.

[5] J. Dong, H. Lim, S. Park, and S. Nam, “Singular wire-driven series elastic actuation with force control for a waist assistive exoskeleton, h-wexv2,” *IEEE/ASME Trans. Mechatron.*, vol. 25, no. 2, pp. 1026–1035, Apr. 2020.

[6] T. Chen, R. Casas, and P. S. Lum, “An elbow exoskeleton for upper limb rehabilitation with series elastic actuator and cable-driven differential,” *IEEE Trans. Robot.*, vol. 35, no. 6, pp. 1464–1474, Dec. 2019.

[7] P. J. Besl and H. D. Mckay, “A method for registration of 3-D shapes,” *IEEE Trans. Pattern Anal. Mach. Intell.*, vol. 14, no. 2, pp. 239–256, Feb. 1992.

[8] J. Kim et al., “Reducing the metabolic rate of walking and running with a versatile, portable exosuit,” *Science*, vol. 365, no. 6454, pp. 668–672, 2019.

[9] A. Goto, T. Murase, H. Moritomo, K. Oka, K. Sugamoto, and H. Yoshikawa, “Three-dimensional in vivo kinematics during elbow flexion in patients with lateral humeral condyle nonunion by an image-matching technique,” *J. Shoulder Elbow Surg.*, vol. 23, no. 3, pp. 318–326, 2014.

[10] A. Goto et al., “In vivo three-dimensional wrist motion analysis using magnetic resonance imaging and volume-based registration,” *J. Orthopaedic Res.*, vol. 23, no. 4, pp. 750–756, 2010.

[11] A. C. De Oliveira, J. S. Sulzer, and A. D. Deshpande, “Assessment of upper-extremity joint angles using harmony exoskeleton,” *IEEE Trans. Neural Syst. Rehabil. Eng.*, vol. 29, pp. 916–925, 2021.

[12] N. Vitiello et al., “NEUROExos: A powered elbow exoskeleton for physical rehabilitation,” *IEEE Trans. Robot.*, vol. 29, no. 1, pp. 220–235, Feb. 2013.

[13] D. Park, S. Toxiri, G. Chini, C. Di Natali, D. G. Caldwell, and J. Ortiz, “Shoulder-sideWINDER (shoulder-side wearable INDustrial ergonomic robot): Design and evaluation of shoulder wearable robot with mechanisms to compensate for joint misalignment,” *IEEE Trans. Robot.*, vol. 38, no. 3, pp. 1460–1471, Jun. 2022.

[14] R. W. Jackson and S. H. Collins, “Heuristic-based ankle exoskeleton control for co-adaptive assistance of human locomotion,” *IEEE Trans. Neural Syst. Rehabil. Eng.*, vol. 27, no. 10, pp. 2059–2069, Oct. 2019.

[15] W. Hang et al., “A new kinematics method of determing elbow rotation axis and evaluation of its feasibility,” *J. Peking Univ. (Health Sci.)*, vol. 48, no. 2, pp. 218–223, 2016.

[16] A. Assi, Z. BaKouny, M. Karam, A. Massaad, W. Skalli, and I. Ghanem, “Three-dimensional kinematics of upper limb anatomical movements in asymptomatic adults: Dominant vs. non-dominant,” *Hum. Movement Sci.*, vol. 50, pp. 10–18, 2016.

[17] M. Bottlang, S. M. Madey, C. M. Steyers, J. L. Marsh, and T. D. Brown, “Assessment of elbow joint kinematics in passive motion by electromagnetic motion tracking,” *J. Orthopaedic Res.*, vol. 18, pp. 195–202, 2000.

[18] K. Aouaidjia, B. Sheng, P. Li, J. Kim, and D. D. Feng, “Efficient body motion quantification and similarity evaluation using 3-D joints skeleton coordinates,” *IEEE Trans. Syst., Man, Cybern. Syst.*, vol. 51, no. 5, pp. 2774–2788, May 2021.

[19] Z. Zhang, “Microsoft kinect sensor and its effect,” *IEEE MultiMedia*, vol. 19, no. 2, pp. 4–10, Feb. 2012.

[20] A. Adikrishna, A. L. Kekatpure, J. Tan, H. J. Lee, M. F. Deslivia, and I. H. Jeon, “Vortical flow in human elbow joints: A three dimensional computed tomography modeling study,” *J. Anatomy*, vol. 225, no. 4, pp. 390–394, 2015.

[21] F. Iachello, *Lie Algebras and Lie Groups*. Berlin, Germany: Springer, 2015.

[22] J. S. Dai, “An historical review of the theoretical development of rigid body displacements from rodrigues parameters to the finite twist,” *Mechanism Mach. Theory*, vol. 41, no. 1, pp. 41–52, 2006.

[23] A. Mueller, “Modern robotics: Mechanics, planning, and control [bookshelf],” *IEEE Control Syst. Mag.*, vol. 39, no. 6, pp. 100–102, Dec. 2019.

[24] M. Conconi, N. Sancisi, and V. Parenti-Castelli, “Prediction of individual knee kinematics from an MRI representation of the articular surfaces,” *IEEE Trans. Biomed. Eng.*, vol. 68, no. 3, pp. 1084–1092, Mar. 2021.